Available online at www.sciencedirect.com
SCIENCE DIRECT®
Bioelectrochemistry 59 (2003) 99–106
Bioelectrochemistry
www.elsevier.com/locate/bioelechem

Time evolution of the formation of different size cationic liposome–polyelectrolyte complexes

F. Bordi, C. Cametti*, T. Gili, D. Gaudino, S. Sennato

Dipartimento di Fisica, Universita' di Roma "La Sapienza," Piazzale A. Moro 5 I-00185 Rome, Italy
Istituto Nazionale per la Fisica della Materia (INFM), Unita' di Roma 1, Rome, Italy

Received 23 September 2002; received in revised form 3 January 2003; accepted 13 January 2003

Abstract

We report on the time evolution of the aggregation behaviour of cationic liposome–polyelectrolyte complexes studied by means of dynamic light scattering technique. Pure dioleoyltrimethilammoniumpropane (DOTAP) and mixed DOTAP–dipalmitoylphosphatidylcholine (DPPC) liposomes in polyacrylate sodium salt aqueous solutions in a wide concentration range have been investigated and the size and size distributions of the resulting aggregates evaluated from the intensity autocorrelation function of the scattered light. Under appropriate conditions, we found two discrete aggregation regimes, resulting in two different structural arrangements, whose time evolution depends on the charge ratio and the polyelectrolyte molecular weight. A first small component of average size in the 100–500 range nm coexists with a larger component, whose typical size increases with time, up to some micrometers. The cluster growth from a single liposome, 70 nm in diameter, to the formation of polymer-coated liposome aggregates has been briefly discussed in the light of steric stabilization of colloids. Moreover, it has been found that the kinetics of aggregation of the larger, time-dependent, component follows a dynamical scaling within the diffusion-limited cluster aggregation (DLCA) regime. The understanding of structures resulting from interactions between polyelectrolytes with oppositely charged liposomes may help towards formulation of "lipoplexes" (cationic lipid–DNA complexes) to use as non-viral gene carriers.

Keywords: DOTAP; DPPC; Aggregation

1. Introduction

Complexation of a polyelectrolyte with oppositely charged, spheroidal particles (liposomes and micelles) has received for some years now great attention and has been subject of theoretical and experimental researches [1]. An extensive review on this subject has been given by Park et al. [2]. This phenomenon, which plays an important role in many aqueous solutions of biological objects, is of special interest in gene therapy, where the complexation of DNA with positively charged liposomes—thereby making the contact with an usually negative cell membrane more likely—has been intensively investigated [3–5]. Owing to the complexity of self-assembly, it is reasonable to expect a hierarchical self-assembled variety of structures, including clusters of aggregated particles, polymer-coated particles, tubular and lamellar or multilamellar structures, each of them characterized by a broad size distribution. However, their influence on the desired biological activity has yet to be properly defined, and there is a lack of complete characterization of the physico-chemical parameters involved, despite the fact that, for biomedical application, the stability, shape and size distribution of the complexes are important. In fact, the size of lipoplexes is found to be determinant in their transfection effectiveness since aggregation has been recognized as the reason for the transfection efficacy loss in liquid formulation with the increase of the lipoplex size [6].

Moreover, in spite of extensive efforts in both theoretical and experimental investigations carried out in the last decade, a clear definition of the role of the parameters governing the complex formation and their different structures is poorly understood and, surprisingly, little attention

* Corresponding author. Dipartimento di Fisica, Universita' di Roma "La Sapienza," Piazzale A. Moro 5 I-00185 Rome, Italy. Tel.: +39-06-49913476; fax: +39-06-4463158.
E-mail address: cesare.cametti@roma1.infn.it (C. Cametti).

1567-5394/03/$ - see front matter © 2003 Elsevier Science B.V. All rights reserved.
doi:10.1016/S1567-5394(03)00007-0

has been given to the stability of polyelectrolyte self-assemblies, where interactions with polyions can result in phase separation and structural rearrangements.

For example, cationic lipids forming liposomes when mixed with DNA form a self-assembling supramolecular complex (lipoplex) exhibiting a large variety of different structures, whose temporal formation can be summarized as follows [7,8]. Starting from liposomal vesicles 50–100 nm in diameter, after DNA addition, spherical structures (lipoplexes) in the range of 200–500 nm with a relatively narrow size distribution are formed, to which it follows the formation of larger complexes, whose size increases with time up to values of the order of 1–5 μm. The structural transformation occurring in these systems have been attributed to processes involving bilayer rupture and fusion [9]. Due to thermodynamic instability, these structures have the tendency to grow into larger aggregates over time, giving rise to clusters of aggregated liposomes, tubular and multilamellar structures, all of them highly heterogeneous with a broad size distribution. Interestingly, the fraction of small lipoplexes remains. Anionic liposomes mixed to polycations behave similarly [10], providing further evidence that electrostatic interactions are mainly responsible for liposome aggregation and complex formation.

This is an unusual behaviour when compared to the aggregation phenomena occurring in typical charge-stabilized colloidal particles, where—in order to reduce the electrostatic repulsion component—it follows the formation of a cluster of continuously increasing size, which tends to result in an infinite cluster, for a long time limit.

In the context of cationic liposome and nucleic acids interactions, physical transformations yielding new colloids are still poorly defined [11,12]. A relatively simpler system is found if the biological polyelectrolyte, such as DNA, is substituted with a synthetic polyion.

This paper is aimed at determining the phenomenological behaviour of the time evolution of the structure and the stability of charged colloidal particles in the presence of oppositely charged polyions, which play, at a mesoscopic scale, the role of small counterions in the salt-induced aggregation of charge-stabilized hydrophobic colloids [13].

In this work, we investigated via dynamic light scattering measurements the formation of aggregates resulting from interactions of cationic liposomes with a linear flexible polyanion of different molecular weights and at different concentrations in the bulk aqueous phase. We used liposomes built up of two different lipids, DPPC, a zwitterionic lipid, and DOTAP, a positively charged lipid, and mixed DOTAP–DPPC liposomes dispersed in an aqueous phase. As polyelectrolyte, we employed polyacrylate sodium salt (NaPAA) of different molecular weights (5.1, 60 and 225 kDa) in a wide concentration range to cover, in the bulk solution, different concentration regimes—from semidilute unentangled to concentrated regime.

We have found two different regimes, resulting in two coexisting well-characterized structures of different sizes, and the influence of polyion concentration, molecular weight and polyion–liposome charge ratio was investigated and is briefly discussed.

2. Experimental

2.1. Liposome preparation

Dioleoyltrimethilammoniumpropane (DOTAP) and dipalmitoylphosphatidylcholine (DPPC) were purchased from Avanti Polar Lipids (Alabaster, AL) and used without further purification.

Appropriate amount of DOTAP or mixed DOTAP–DPPC at the desired mole ratio was dissolved in a methanol–chloroform mixture (1:1 vol/vol) and the solution was placed in a glass vessel and allowed to form a dry film after rotary evaporation of the solvent under vacuum overnight. The film was then hydrated with 10 ml pure water at the temperature of 42 °C for 1 h. The resulting mixture was sonicated at a temperature of 25 °C for 1 h at continuous power mode using a probe sonicator model Vibra-Cell Sonics, until the solution appeared to be optically transparent in white light. A homogeneous liposomal suspension of unilamellar vesicles was obtained. The liposome suspension was then filtered through a 0.45-μm polycarbonate filter (Millipore). Polyacrylate sodium salt [NaPAA] of different molecular weights (5.1, 60 and 225 kDa) was obtained from Polyscience. Polydispersity was $M_w/M_n < 1.3$ for all the polymers investigated. Polyelectrolyte solutions were prepared with distilled and deionized water of low ionic conductivity (less than 1–2 μS/cm).

It was previously found [14,15] that the order of mixing liposome and polymer components could affect the size and size distribution of the different structures present in the mixed suspension. In this light, the polymer solution at the appropriate concentration (in all experiments) was added to the liposome suspension, whose lipid concentration was kept constant at about 1 mg/ml.

For all the molecular weights investigated, the viscosity of polymer solutions employed has been measured at 25 °C in a wide concentration range, and these values have been used to correlate, through the Stokes–Einstein relationship, the translational diffusion coefficient D_T, obtained from the dynamic light scattering measurement, to the particle hydrodynamic radius R_H.

2.2. Dynamic light scattering measurements

Due to the Brownian motion of particles moving in the solution, scattered light fluctuates in intensity. The homodyne intensity–intensity correlation function $g^{(2)}(q,t)$ was measured at a scattering angle of 90° with a Brookhaven (BI-9000AT) digital correlator using a laboratory-built setup equipped with a 10-mW He–Ne laser. For a Gaussian distribution of the intensity profile of the scattered light,

$g^{(2)}(q,t)$ is related to the electric field correlation function $g^{(1)}(q,t)$ by

$$g^{(2)}(q,t) = A(1 + B(g^{(1)}(q,t))^2) \quad (1)$$

where A and B are the experimental baseline and the constant depending on the optic system, respectively, and $g^{(1)}(q,t)$ is given by

$$g^{(1)}(q,t) = \int_0^\infty G(\Gamma)\exp(-\Gamma t)\mathrm{d}\Gamma. \quad (2)$$

Here, $G(\Gamma)$ is the normalized number distribution function for the decay constant $\Gamma = q^2 D_T$ where $q=(4\pi n/\lambda)\sin(\theta/2)$ is the scattering vector, n is the refractive index of the medium and D_T is the traslational diffusion coefficient related to the hydrodynamic radius R_H by the Stokes–Einstein relationship

$$D_T = \frac{k_B T}{6\pi\eta R_H} \quad (3)$$

where $k_B T$ is the thermal energy and η is the viscosity of the medium. For systems having a narrow size distribution, the diffusion coefficients of aggregates were determined by fitting the data using a cumulant expansion [16,17] given by

$$\ln(g^{(1)}(q,t)) = -q^2\langle D_T\rangle t + 1/2\mu_2 q^4 t^2 + O(t^3) \quad (4)$$

where $\langle D_T\rangle$ is the mean of the diffusion coefficient and μ_2 is the variance of the distribution, with a measure of the polydispersity given by

$$Q^2 = \frac{\mu_2}{\langle D_T\rangle^2}. \quad (5)$$

For systems having polydispersity, intensity-weighted distributions of the hydrodynamic radii were determined from the autocorrelation function using a Laplace inversion routine, which employs the constrained regularization method (CONTIN program) [18], searching for the smoothest non-negative solution for $G(\Gamma)$ that is consistent with the experimental data. More detailed information about the size distribution of polydisperse systems by means of a Laplace inversion of the correlation function can be found elsewhere [19–23].

3. Results and discussion

An example of size distribution as measured by dynamic light scattering of sonicated and 0.45-μm filtered DOTAP liposomes is given in Fig. 1. Mixed DOTAP–DPPC liposomes behave similarly. The average diameter was found to be around 80 nm; this value is constant over long period of time, up to days or weeks. A typical correlation function of the normalized scattered electric field is shown in the inset of Fig. 1.

We investigated the time evolution of complexes formed by DOTAP or DOTAP–DPPC liposomes in the presence of

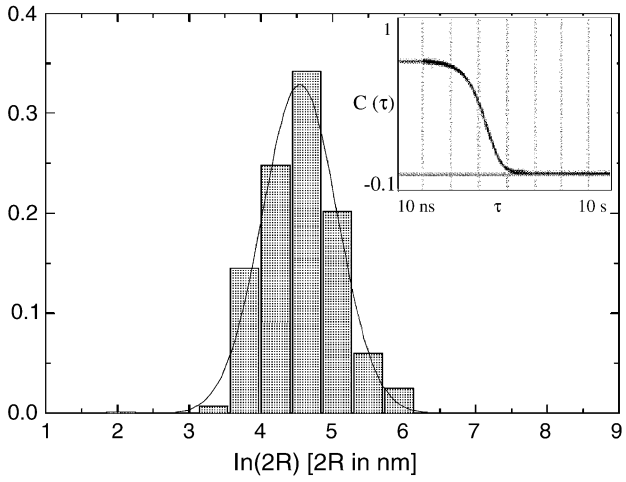

Fig. 1. A histogram of the average diameter of the unimodal distribution of DOTAP liposomes as determined by dynamic light scattering data. The full line is calculated on the basis of a log-normal distribution. In the inset, a typical normalized autocorrelation function $g^{(1)}(t)$, fitted according to a second-order cumulant expansion (Eq. (4)) is shown.

negatively charged polyelectrolytes (polyacrylate sodium salt) of different molecular weights and at different bulk concentrations. The kinetics of this complex formation involves at least two different mechanisms, resulting, in some cases, in the simultaneous presence of two well-differentiated structures, the typical sizes of which lie in the range 100–500 nm and 1–5 μm, respectively.

The time evolution of these two aggregates are shown in Figs. 2–4 for DOTAP liposomes in the presence of NaPAA of molecular weights 5.1, 60 and 225 kDa, respectively, at different polymer concentrations. Similar dependencies are shown in Figs. 5 and 6 for the mixed DOTAP–DPPC liposome systems, in the presence of the same polyelectrolyte.

In order to characterize the various structures in the different experimental conditions investigated, we introduce, following Radler et al. [24], two dimensionless parameters, $L/P=(L^+ + L^0)/P$, defined as the lipid (L)-to-polyelectrolyte (P) mass ratio, where L^+ and L^0 are the weight of the cationic and the zwitterionic lipids, and the parameter ξ defined as the lipid to polyelectrolyte charge ratio

$$\xi = \frac{L^+}{M_w(L^+)}\frac{M_w(P_{mon})}{P} \quad (6)$$

where $M_w(L^+)$ and $M_w(P_{mon})$ are the molecular weights of the charged lipid and polyion monomer, respectively.

In the presence of polymers of low molecular weight ($M_w = 5.1$ kDa), the resulting aggregates are stable up to a charge ratio of about $\xi = 0.004$ (excess of polyelectrolyte charge) and only at lower values of ξ there is an increase in the aggregate average size, that, starting from 100 to 200 nm, reaches at long time values of around 1 μm.

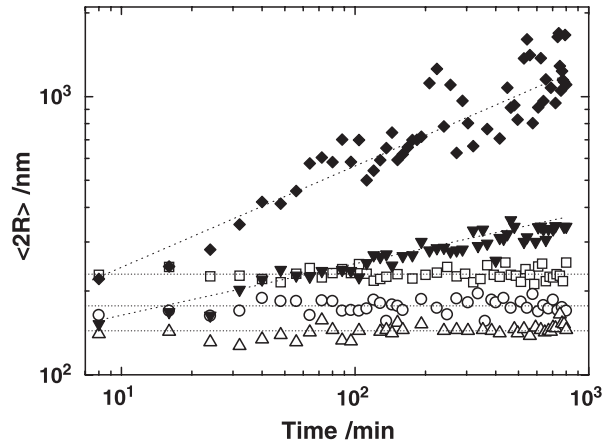

Fig. 2. The time evolution of the average diameter $\langle 2R \rangle$ of DOTAP–NaPAA complexes for different values of the charge ratio ξ: (□) $\xi \approx 0.25$; (○) $\xi \approx 0.025$; (△) $\xi \approx 0.004$; (▼) $\xi \approx 0.002$; (♦) $\xi \approx 0.0015$. The polymer molecular weight is $M_w = 5.1$ kDa. The average diameters are derived from the CONTIN analysis and, for all the samples investigated, a monomodal size distribution is observed.

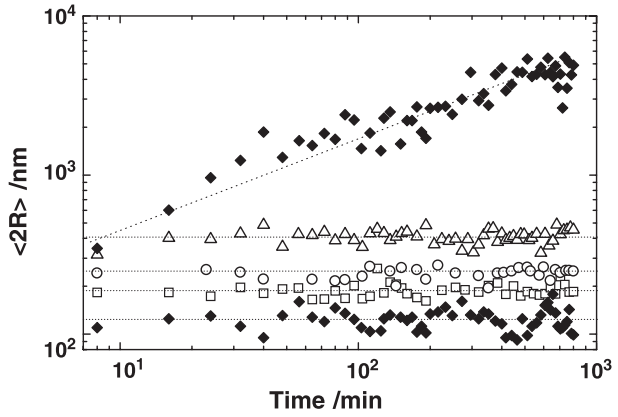

Fig. 4. The time evolution of the average diameter $\langle 2R \rangle$ of DOTAP–NaPAA complexes for different values of the charge ratio ξ: (□) $\xi \approx 8.1$; (○) $\xi \approx 3.9$; (△) $\xi \approx 1.9$; (♦) $\xi \approx 0.2$. The polymer molecular weight is $M_w = 225$ kDa. The average diameters are derived from the CONTIN analysis. In this case, we observe a unimodal size distribution for $\xi \geq 1.9$ and a bimodal distribution for $\xi = 0.2$ (both peak—indicated by the symbol (♦)—of the two distributions are shown).

In all of these systems, we observe a relatively narrow monomodal distribution well described by a log-normal distribution [21]

$$f(R) = \frac{\exp(-\delta^2/2)}{\sqrt{2\pi} R_0 \delta} \exp\left(-\frac{\ln R - \ln R_0}{2\delta^2}\right) \quad (7)$$

where R_0 is the peak value and δ is related to the relative variance σ^2 by $\delta^2 = \ln(1+\sigma^2)$.

In the presence of polymer with higher molecular weight ($M_w = 60$ and 225 kDa), the stable monomodal size distribution structure is maintained over a wider range of ξ values; however, beside these values, a bimodal distribution appears with the component of smaller size stable as a function of time and that of larger size continuously increasing with time, up to the formation of large flocs. A typical behaviour is depicted in Fig. 7, where the log-normal distributions of the liposome size at a given time during the aggregation process, for different values of ξ, are shown. As can be seen, at $\xi < 1$, the distribution splits into two well-separated distributions corresponding to the stable and the time-increasing structure, respectively. It worthy to note that this peculiar phenomenology depends on the polymer molecular weight, so that the stability of the system is governed not only by the charge ratio ξ but also by this parameter. A schematic view of the extension of the region

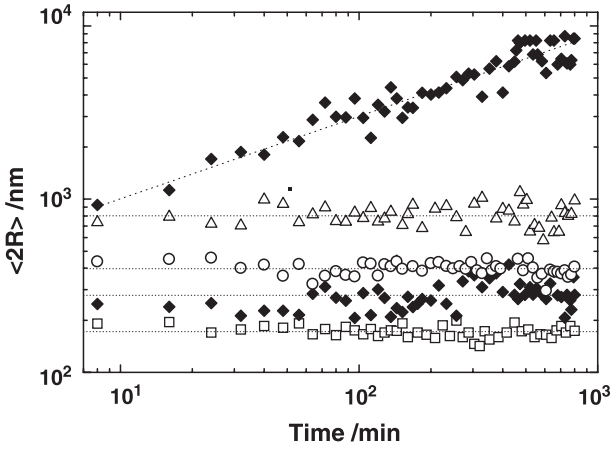

Fig. 3. The time evolution of the average diameter $\langle 2R \rangle$ of DOTAP–NaPAA complexes for different values of the charge ratio ξ: (□) $\xi \approx 7.5$; (○) $\xi \approx 1.9$; (△) $\xi \approx 0.2$; (♦) $\xi \approx 0.13$. The polymer molecular weight is $M_w = 60$ kDa. The average diameters are derived from the CONTIN analysis. In this case, we observe a unimodal size distribution for $\xi \geq 0.2$ and a bimodal distribution for $\xi = 0.13$ (both peaks—indicated by the same symbol (♦)—of the two distributions are shown).

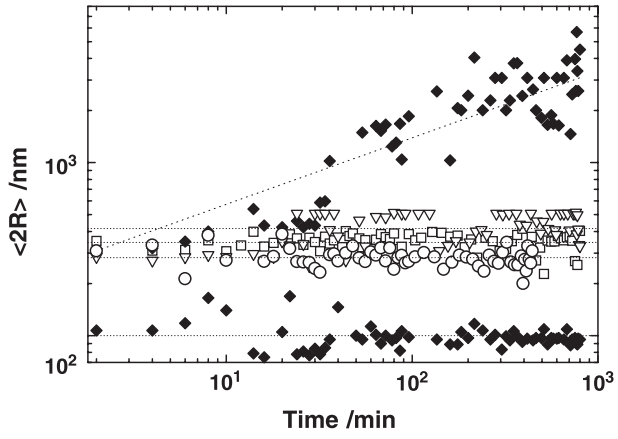

Fig. 5. The time evolution of the average diameter $\langle 2R \rangle$ of mixed DOTAP–DPPC liposomes (0.6:0.4 wt/wt) in the presence of NaPAA of molecular weight 60 kDa, for different values of the charge ratio ξ: (□) $\xi \approx 2.0$; (○) $\xi \approx 0.04$; (♦) $\xi \approx 0.02$; (▽) $\xi \approx 0.002$. The average diameters are derived from the CONTIN analysis. Also in this case, we observe a unimodal size distribution for $\xi \geq 0.04$ and a bimodal distribution for $\xi = 0.02$ (both the peak (indicated by the same symbol (♦) of the two distributions are shown). At very high polymer concentration ($(L^+ + L^0)/P = 0.002$), a new unimodal distribution appears.

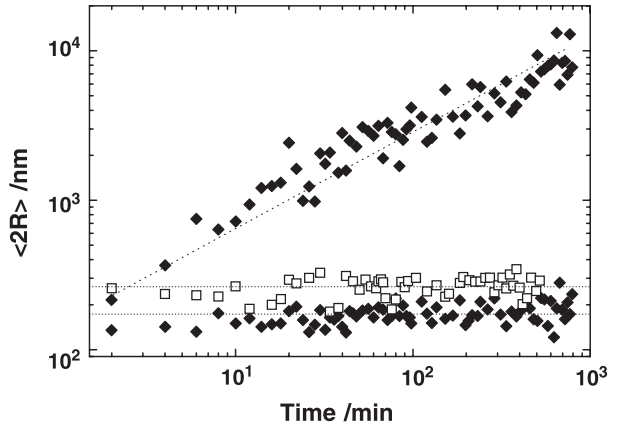

Fig. 6. The time evolution of the average diameter $\langle 2R \rangle$ of mixed DOTAP–DPPC liposomes (1.6 molar ratio) in the presence of NaPAA of molecular weight 225 kDa, for different values of the charge ratio ξ: (□) $\xi \approx 2.0$; (♦) $\xi \approx 0.08$; The average diameters are derived from the CONTIN analysis. We observe a unimodal size distribution for $\xi \geqslant 2.0$ and a bimodal distribution for $\xi = 0.08$. In this case, both peaks—indicated by the same symbol (♦)—of the two distributions are shown.

of the stable, small size, aggregate and the unstable larger size structures for various values of the charge ratio ξ and molecular weight is shown in Fig. 8.

The simultaneous presence of two kinds of structures is unusual in the typical behaviour of charge-stabilized colloidal suspensions, where the reduction of the electrostatic interactions yields to a cluster formation with a unique size distribution, continuously spreading with time, until an infinite cluster fills the whole system.

As far as the first component is concerned, the aggregation mechanism can be rationalized in the following scheme. In the low polyion concentration regime, NaPAA polymer is adsorbed onto the liposome surface. Liposome collision promotes bridging, leading to the formation of globules which include few liposomes. The adsorbed layer thickness d depends on the polymer molecular weight M_w, according to the scaling relationship [25–28]

$$d = R_H - R_{H0} = aM_w^v \quad (8)$$

where R_H and R_{H0} are the hydrodynamic radii of polymer-coated and bare liposome particle, respectively, and v is an exponent varying between 0.5 and 1. The prefactor a indicates the monomer size. Within this framework, it is noteworthy that, within defined polymer concentrations, the exponent v approximately assumes the same value, independently of the charge ratio. At higher concentrations, a gradual desorption occurs, inducing a depletion flocculation. Hydrophobic association between chains, which are adsorbed on the particle surface, leads to the formation, upon particle collision, of a dimeric aggregate [29]. This basic structure is stable until, with the increase of the polymer concentration, the polymer–solvent interactions prevail upon hydrophobic interactions and isolated polymer-coated liposomes are newly favoured. When the polymer concentration is further increased, a heavy coverage of the liposome surface causes a depletion stabilization.

A schematic view of the evolution of the possible aggregation process is depicted in Fig. 9 where, together with the values of the exponent v deduced from Eq. (8) in the different polyion concentration ranges, we sketched the possible structural arrangement of the resulting aggregates.

When the charge ratio decreases (excess of polymer charge) and the polymer molecular weight increases, the second component, whose average size increases, appears. Fig. 8 shows the region of existence of both the "stable" and "unstable" aggregates, as a function of ξ and M_w, in the

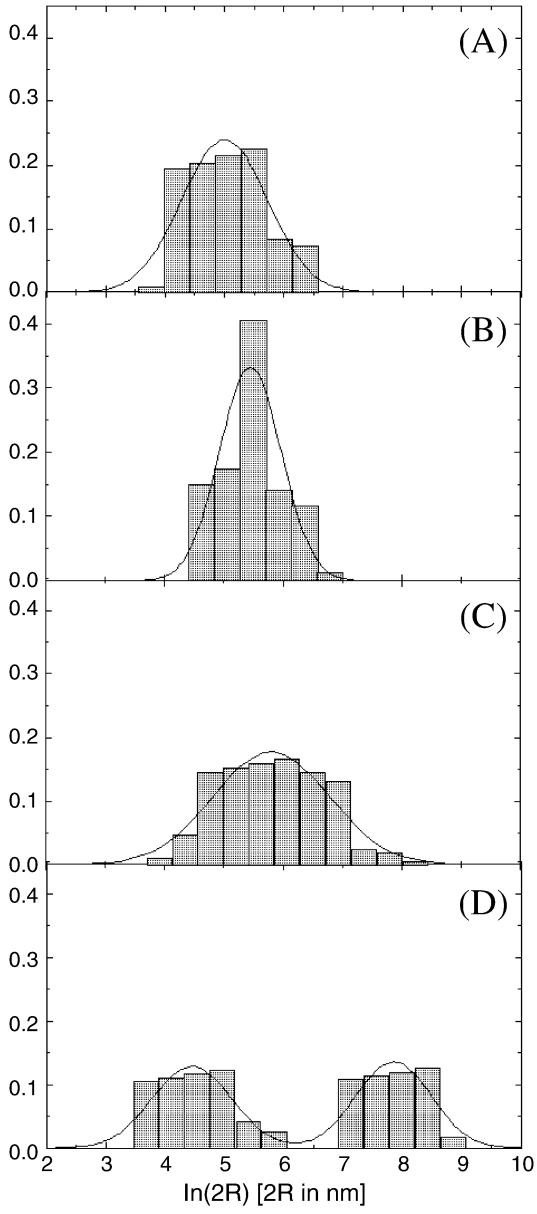

Fig. 7. The histogram of the size distribution of DOTAP liposomes in the presence of NaPAA of molecular weight $M_w = 225$ kDa, at different charge ratios ξ: (A) $\xi = 8.1$; (B) $\xi = 3.9$; (C) $\xi = 1.9$; (D) $\xi = 0.2$. The full lines are calculated on the basis of a log-normal distribution. The data refer to a given time ($t = 400$ min) from the beginning of the aggregation process.

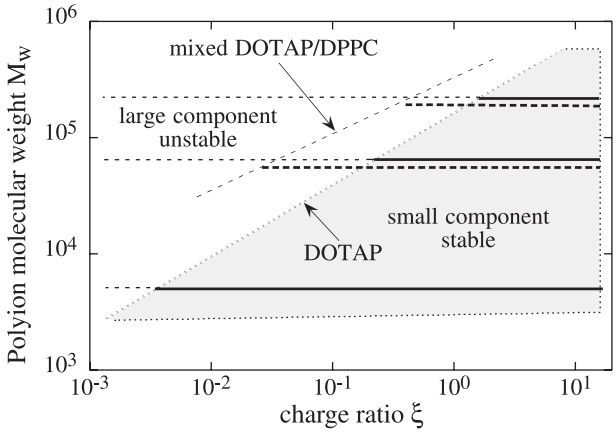

Fig. 8. The region of existence of the "small" component and "large" component for pure DOTAP (full line) and mixed DOTAP–DPPC (0.6:0.4 wt/wt) (dotted line) in the presence of NaPAA of different molecular weights and for different charge ratios.

range investigated. It is noteworthy that, in the case of mixed DOTAP–DPPC liposomes, the boundary above which the increasing component appears, is shifted towards higher molecular weight values, suggesting a fine interplay between the liposome surface charge and the polymer conformation in the bulk solution.

We have recently measured [30] the viscosity of NaPAA aqueous solutions in a wide concentration range and have observed three different regimes characterized by different exponents in the viscosity–concentration scaling law

$$\eta \approx C^{\alpha} \tag{9}$$

which corresponds to regions with different polymer conformations, i.e., semidilute unentangled regime (with exponent 1/2), semidilute entangled regime (with exponent 3/2) and concentrated regime (with exponent 15/4). The concentrations at which the different regimes occur are approximately $C=0.03-0.04$ and $0.1-0.15$ g/ml for semidilute unentangled–entangled and entangled–concentrated regime, respectively. These values compare reasonably well with those for which we observe, for the two higher molecular weights investigated, with the presence of a large size, time-dependent, component. For NaPAA with a molecular weight $M_w=5.1$ kDa, the transition from entangled and concentrated regime is shifted towards higher values, in agreement with the finding from dynamic light scattering measurements, where the beginning of the cluster growth occurs for $L^+/P>0.015$, corresponding to a charge ratio $\xi>0.002$.

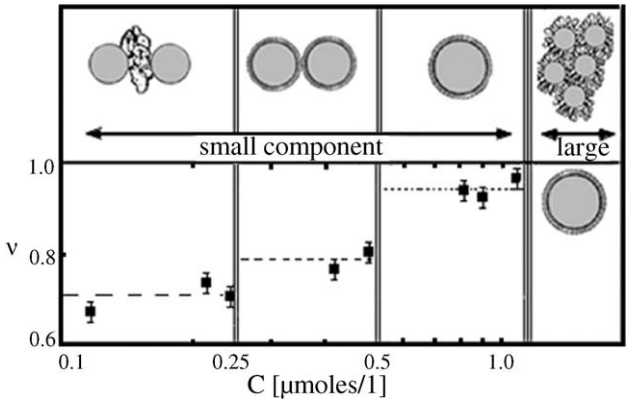

Fig. 9. The exponent assumes ν of Eq. (8) as a function of the NaPAA concentration for pure DOTAP and mixed DOTAP–DPPC liposomes. Three different regions are evidenced to which correspond three typical aggregates (monomodal size distribution) whose hypothetical structure are also sketched. At concentration higher than 1 μmol/l, a bimodal distribution appears and large, time-dependent, aggregates coexist with small stable aggregates.

As far as the second, time-dependent, component is concerned, flocs held together by polymer chains undergo a reorganization resulting in the formation of clusters that comply with a fractal morphology. The kinetics of aggregation is, as usual, described by dynamical scaling [31,32], and the time evolution of the average hydrodynamic radius of the resulting clusters is given by

$$R_H(t) = R_H(0)\left(\frac{t}{t_0}\right)^{\beta} \tag{10}$$

where $\beta=z/D$, with D as the fractal dimension of the cluster and z as the kinetic exponent.

The value of the parameter β for DOTAP and mixed DOTAP–DPPC liposome suspensions in the presence of NaPAA of different molecular weights and in the concentration range of 1–100 mg/ml is shown in Fig. 10. As can be seen, when the lipid/polyelectrolyte charge ratio ξ and/or the lipid/polyelectrolyte mass ratio, L/P, allows the presence of a component whose size increases with time, the β data scatter around the value predicted in the diffusion-limited cluster aggregation (DLCA) regime, assuming for the fractal

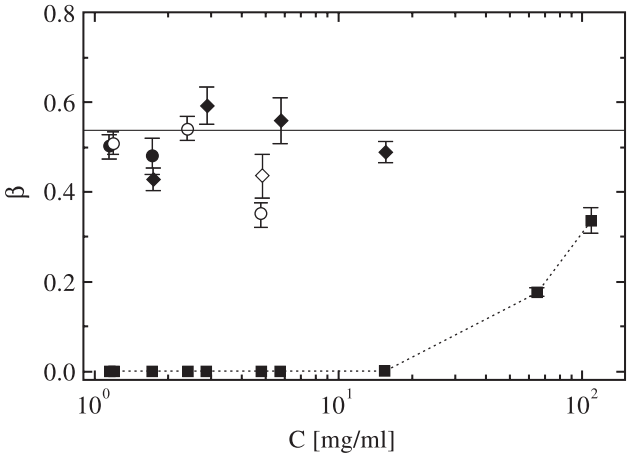

Fig. 10. The kinetic exponent β of the power-law dependence of the hydrodynamic radius as a function of time for pure DOTAP and mixed DOTAP–DPPC liposomes in the presence of NaPAA of different molecular weights. The data are plotted as a function of the polymer concentration: (○) DOTAP–DPPC (0.6:0.4 wt/wt), $M_w=225$ kDa; (◇) DOTAP–DPPC (0.6:0.4 wt/wt), $M_w=60$ kDa; (●) DOTAP; $M_w=225$ kDs; (◆) DOTAP; $M_w=60$ kDa; (■) DOTAP; $M_w=5.1$ kDa. The dotted line represents the calculated value assuming the fractal dimension of the cluster $D_f=1.86$.

dimension D the value of $D = 1.86$ [31,32]. It must be noted, however, that liposomes in the presence of NaPAA of low molecular weight ($M_w = 5.1$ kDa) behave differently, the exponent β being zero (stable size distribution) at low polyion concentration and increasing towards the expected value at higher polyion concentrations. These results show that the cluster growth kinetics can be described at long times by power laws, except for the lowest molecular weight polyion, in the low concentration regime, where the aggregate growth is absent.

4. Conclusions

The cluster growth observed in this work can be summarized in the framework of the following scenario. Liposome–polyelectrolyte interactions give rise to two different structures of different typical size:

(i) small aggregates of average size between 100 and 500 nm, whose size remains constant as a function of time;
(ii) large clusters (flocculation of lipid–NaPAA complexes) with size of the order of 500 nm or larger, with a continuous time evolution up to structures as large as 5 μm in diameter. The size distribution of these complexes depends strongly on the L/P mass ratio or the charge ratio ξ. The appearance of this second component which increases with time, although common to all the systems investigated, depends on the polymer concentration and molecular weight of the polyelectrolyte, and only above some critical values does this structure form.

This behaviour differs from that observed in salt-induced aggregation of charge-stabilized colloidal particle suspensions, whose kinetics is generally described within the diffusion-limited cluster aggregation (DLCA) or reaction-limited cluster aggregation (RLCA) yielding, at long time, an infinite size cluster [32,33]. In contrast, in the present systems, there is a simultaneous presence of two different types of aggregates, i.e., a stable small-size aggregate and an unstable large-size aggregate, whose growth behaviour is reminiscent of that observed in usual charged colloidal systems. It is noteworthy that the relative percentage of the two populations are generally comparable, so that two different aggregation processes are present. These characteristics can be relevant in transfection efficiency in the intracellular delivery of nucleic acids, where size stability exerts a major influence. Moreover, the knowledge of the phase diagram relating physico-chemical parameters to the average cluster size of heterogeneously formed complexes would improve transfection efficiency conditions.

References

[1] T.T. Nguyen, B.I. Shklovskii, Overcharging of a macroion by an oppositely charged polyelectrolyte, Physica A 293 (2001) 324–338.
[2] S.Y. Park, R.F. Bruinsma, W.M. Gelbart, Spontaneous overcharging of macro-ion complexes, Europhys. Lett. 46 (1999) 454–460.
[3] J.O. Radler, I. Koltover, T. Salditt, C.R. Safinya, Structure of DNA–cationic liposome complexes: DNA intercalation in multilamellar membranes in distinct interhelical packing regimes, Science 275 (1997) 810–814.
[4] J. Gustafsson, G. Arvidson, G. Karlsson, M. Almgren, Complexes between cationic liposomes and DNA visualized by cryo-TEM, Biophys. Biochim. Acta 1235 (1995) 305–312.
[5] I.S. Zuhorn, D. Hoekstra, On the mechanism of cationic amphiphile-mediated transfection. To fuse or not to fuse. Is that the question? J. Membr. Biol. 183 (2002) 167–182.
[6] E. Lai, J.H. van Zanten, Evidence of lipoplex dissociation in liquid formulation, J. Pharm. Sci. 91 (2002) 1225–1232.
[7] E. Lai, J.H. van Zanten, Real time monitoring of lipoplex molar mass, size and density, J. Control. Release 82 (2002) 149–158.
[8] V. Oberle, U. Bakowsky, I.S. Zuhorn, D. Hoekstra, Lipoplex formation under equilibrium conditions reveals a three-step mechanism, Biophys. J. 79 (2000) 1447–1454.
[9] S. Huebner, B.J. Battersby, R. Grimm, G. Cevc, Lipid–DNA complex formation: reorganization and fusion of lipid bilayers in the presence of DNA as observed by cryo-electron microscopy, Biophys. J. 76 (1999) 3158–3166.
[10] E.K. Wasan, P. Harvie, K. Edwards, G. Karlsson, M.B. Bally, A multi-step lipid mixing assay to model structural changes in cationic lipoplexes used for in vitro transfection, Biochim. Biophys. Acta 1461 (1999) 27–46.
[11] Y. Barenholz, Liposome application: problems and prospects, Curr. Opin. Coll. Interface Sci. 6 (2001) 66–77.
[12] O. Tirosh, Y. Barenholz, Y. Katzhendler, A. Priev, Hydration of polyethylene glycol-grafted liposomes, Biophys. J. 74 (1998) 1371–1379.
[13] J.-P. Hansen, H. Lowen, Effective interactions between electric double layers, Annu. Rev. Phys. Chem. 51 (2000) 209–242.
[14] F. Boffi, A. Bonincontro, F. Bordi, E. Bultrini, C. Cametti, A. Congiu-Castellano, F. De Luca, G. Risuleo, Two-step mechanism in cationic lipoplex formation as observed by dynamic light scattering, dielectric relaxation and circular dichroism methods, Phys. Chem. Chem. Phys. 4 (2002) 2708–2713.
[15] M.T. Kennedy, E.V. Pozharski, V.A. Rakhmanova, R.C. MacDonald, Factors governing the assembly of cationic phospholipid–DNA complexes, Biophys. J. 78 (2000) 1620–1633.
[16] D.E. Koppel, Analysis of macromolecular polydispersity in intensity correlation spectroscopy: the method of cumulants, J. Chem. Phys. 57 (1972) 4814–4820.
[17] C.S. Johnson, D.A. Gabriel, Laser Light Scattering, Dover Publication, New York, 1994.
[18] S.W. Provencher, CONTIN: a general purpose constrained regularization program for inverting noisy linear algebraic and integral equations, Comp. Phys. Commun. 27 (1982) 229–242.
[19] F.R. Hallett, T. Craig, J. Marsh, B. Nickel, Particle size analysis: number distribution from dynamic light scattering, Can. J. Spectrosc. 34 (1989) 63–70.
[20] L. Beney, E. Linares, E. Ferret, P. Gervais, Influence of the shape of phospholipid vesicles on the measurement of their size by photon correlation spectroscopy, Eur. Biophys. J. 27 (1998) 567–574.
[21] A.J. Jin, D. Huster, K. Gawrisch, R. Nossal, Light scattering characterization of extruded lipid vesicles, Eur. Biophys. J. 28 (1999) 187–199.
[22] J. Pencer, G.F. White, F.R. Hallett, Osmotically induced shape changes of large unilamellar vesicles measured by dynamic light scattering, Biophys. J. 81 (2001) 2716–2728.
[23] F.R. Hallett, J. Watton, P. Krygsman, Vesicle sizing. Number distribution by dynamic light scattering, Biophys. J. 59 (1991) 357–362.
[24] J.O. Radler, I. Koltover, A. Jamieson, T. Salditt, C.R. Safinya, Structure and interfacial aspects of self-assembled cationic lipid–DNA gene carrier complexes, Langmuir 14 (1998) 4272–4283.
[25] P.C. Hiemenz, R. Rajagopalan, Principles of Colloid and Surface Chemistry, Marcel Dekker, New York, 1997.

[26] J. Lyklema, Fundamentals of Interface and Colloid Science, Academic Press, San Diego, CA, 1995.
[27] J.A. Baker, J.C. Berg, Investigation of the adsorption configuration of polyethylene oxide and its copolymers with polypropylene oxide on model polystyrene latex dispersions, Langmuir 4 (1988) 1055–1061.
[28] M. Polverari, T.G.M. van de Ven, Dynamic light scattering of PEO-coated latex particles, Colloids Surf. A 86 (1994) 209–228.
[29] E. Dickinson, C. Elvingson, The structure of aggregates formed during the very early stages of colloid coagulation, J. Chem. Soc., Faraday Trans. 2 (84) (1988) 775–789.
[30] F. Bordi, R.H. Colby, C. Cametti, L. De Lorenzo, T. Gili, Electrical conductivity of polyelectrolyte solutions in the semidilute and concentrated regime: the role of the counterion condensation, J. Phys. Chem. B 106 (2002) 6887–6893.
[31] C.M. Sorensen, B.J. Olivier, Variable aggregation rates in colloidal gold: kernel homogeneity dependence on aggregant concentration, Phys. Rev. A 41 (1990) 2093–2100.
[32] C. Cametti, P. Codastefano, T. Tartaglia, Aggregation kinetics in model colloidal systems. A light scattering study, J. Colloid Interface Sci. 131 (1989) 409–422.
[33] G. Bolle, C. Cametti, P. Codastefano, P. Tartaglia, Kinetics of salt-induced aggregation in polystyrene lattices studied by quasielastic light scattering, Phys. Rev. A 35 (1987) 837–841.